

Ultrafast laser excitation of coherent spin waves in exchange-biased IrMn/Co

Keoki Seu* and Anne Reilly

Department of Physics, College of William and Mary, Williamsburg, VA, 23187, USA

(Dated: March 23, 2005)

We have excited and detected coherent spin waves in exchange-biased IrMn/Co systems by ultrafast laser pump-probe magneto-optical Kerr effect (MOKE). Such ultrafast measurements provide opportunity to study the ultimate time scale for these processes as well as determination of fundamental parameters such as anisotropy and damping. This is in analogy with ferromagnetic resonance (FMR), but with the benefit of direct access to the time domain, sub-micron spatial resolution and straightforward in-situ application. These exchange biased IrMn/Co systems are frequently used in magnetic sensors for disk based storage and magnetic random access memory devices (MRAM) for non-volatile storage. The coherent spin waves detected are single frequency, with a frequency which depends strongly on applied magnetic field. The spin waves exist in all orientations, applied fields, and exchange biased field strengths tested. The frequencies were fit to FMR theory using terms for the exchange biasing and demagnetization fields.

The understanding of switching in magnetic systems has become a critical problem in the physics of thin magnetic films. This is an important development step in the formation of magnetic random access memory devices (MRAM), the non-volatile type of RAM where information is stored either in magnetic tunnel junctions or magnetic spin valves. As opposed to conventional RAM where the information is stored in the form of electric potentials MRAM stores the information using magnetic spins, which have the advantage that they require no power to hold the state of the magnetization and will remain in a given state until flipped by a magnetic field. This is a crucial step for new systems, especially space-based satellites where power requirements are an important criteria in choosing technologies. In addition to MRAM, magnetic multi-layers are also important for the design of magnetic sensors, often used in computer guidance systems. With both of these applications, the switching behavior of magnetic spins becomes important since it sets the ultimate timescale for MRAM speeds and sensor response time.¹

I. INTRODUCTION

Ferromagnetic (FM) materials are magnetic materials where the spins of the system are all aligned parallel to each other. Materials such as Co, NiFe, Ni, and CoFe are FM materials. Antiferromagnetic (AF) materials such as IrMn, FeMn, and Ni have adjacent magnetic spins aligned anti-parallel to each other.

When an AF and FM layers are grown on top of each other, the AF layer influences the FM layer causing a biased magnetization direction. This phenomenon is known as exchange-bias, and occurs when an AF and FM layer are grown on top of each other.² To create the exchange-bias, the AF/FM interface is heated up to above the temperature where thermal effects dominate (known as the Néel temperature for AF films). The AF/FM interface is then cooled in a magnetic field, causing the system to reorder itself along the magnetic field

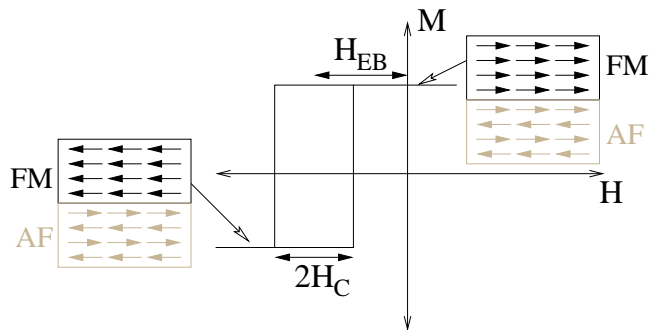


FIG. 1: Hysteresis loop showing the orientation of the FM (black) and AF (brown) as a function of applied field as well as illustrating the coercivity field H_C and exchange bias field H_{EB} .

direction and an anisotropy is formed in the direction of the applied magnetic field. This causes a shift in a magnetic hysteresis loop as seen in Figure 1. The shift is known as the exchange-bias field, H_{EB} . H_{EB} is known to be proportional to $1/t_{FM}$, or the inverse-thickness of the FM layer.²

These material systems are used in magnetic spin valves and tunnel junction devices to give control over the magnetization state. Even though exchange-biasing is used in these devices, the phenomenon is not well understood.^{3,4}

The recent discovery of optical control of magnetization processes has generated a considerable amount of work in understanding the switching behavior and processes in magnetic systems.⁵⁻⁹ In one type of experiment, spin waves are excited by a pulsed magnetic field generated by an ultrafast optical switch.¹⁰ In another type of experiment, spin waves are excited directly by a pulsed laser beam incident on the sample. It has been demonstrated that coherent spin waves could be excited in this way in any ferromagnetic thin film with anisotropy, in the proper geometry. The optically induced spin waves have been shown to give analogous information to ferromagnetic resonance (FMR) and Brill-

loun light scattering (BLS), such as spin wave frequency and damping parameters.⁷

The benefit of the optical experiments are direct access to the time domain, sub-micron spatial resolution, straightforward in-situ application, the ability to study samples in any geometry, and the opportunity for optical control of magnetic processes.

The method of probing the switching behavior in exchange biased systems using ultrafast techniques was first introduced by Ju et. al.^{5,6} on NiFe/NiO. In these experiments, the pump beam was directed via the back of the sample and the optical transparency of NiO was used to directly excite the NiO/NiFe interface. Their results indicate that coherent rotation can be induced in an exchange biased magnetic sample and that the behavior can be modeled using the Landau Lifshitz Gilbert (LLG) equation. Subsequent experiments by Weber et. al.¹¹ on NiFe/FeMn, IrMn/CoFe, and NiMn/CoFe experimentally verified the exponential recovery of the exchange bias as well as correlated the magnetic oscillations with a shifts of the hysteresis loop.

In both of these experiments, however, once the applied magnetic field is large enough to pull all of the magnetization into the direction of the applied field the oscillations disappear, as the minimum energy state is when the magnetization is saturated. There is no ‘kick’ for the magnetization to induce oscillations.⁶

Subsequent studies by van Kampen et. al. on FM NiFe and Ni using a configuration where the film is canted slightly off axis have shown that the pump-probe technique can be used to reproduce equilibrium properties such as FMR frequencies and line widths.⁷

We have optically excited and detected single-frequency coherent spin waves in exchanged-biased IrMn/Co thin films. We have studied the spin wave frequency and damping as a function of applied field and exchange bias field strength. We find that single frequency oscillations on various applied fields and angles, including applied fields past saturation and on the easy axis. The oscillations are fit using FMR models and the extracted H_{EB} and H_D are comparable to measured values.

II. EXPERIMENTAL PROCEDURE

Samples were prepared using dc magnetron sputtering on Si (100) / thermal-oxide substrate. The base pressure was 5×10^{-10} Torr and the background Ar pressure during deposition was 2 mTorr. A 50 Å W and a 50 Å Cu layer were first grown to promote fcc growth of the 100 Å IrMn (AF) and X Co (FM) layers (X=120, 250 Å) and a capping layer of 25 Å Al₂O₃ was used to protect from oxidation. The samples were field cooled from 250° in an applied magnetic field of 100 Oe to pin the magnetization and induce exchange biasing.

The experimental setup is a pump-probe setup using the magneto-optical Kerr effect (MOKE) for magnetization detection. A pulsed Ti:Sapphire laser (Spectra

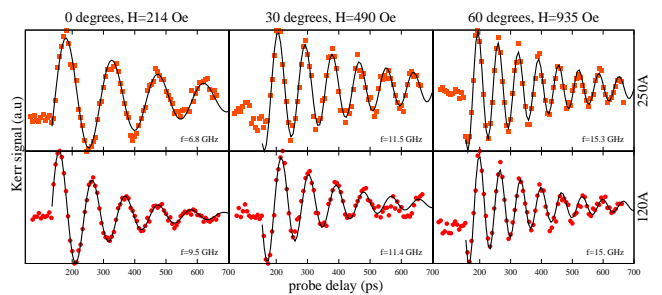


FIG. 2: Example plots of the pump-probe MOKE signal as a function of pump-probe delay for two samples, 250 Å Co (top, orange squares) and 120 Å Co (bottom, red circles) at three different orientations and applied fields. The left column is 0 degrees and 214 Oe, middle column is 30 degrees and 490 Oe, and right column is 60 degrees and 935 Oe. Inset are the frequencies extracted from the fits. The oscillation frequencies from the fits (shown in black) are at the bottom of each plot.

Physics Tsunami) is amplified with a regenerative amplifier (Spectra Physics Spitfire) giving 800 nm output pulses of ~ 150 fs wide with a 1 kHz repetition rate. The beam is split by beam-splitter for the pump and probe beams. The probe beam is delayed using a motion stage so that it arrives some time after the pump beam. The power of the pump beam is on average 10 times the power of the probe beam. Both beams are directed onto the sample which sits in between the poles of a magnet with the pinning axis perpendicular to the optical plane. The angle between the applied field and the exchange bias axis of the sample can be rotated in any direction. The spot size of the pump is ~ 3 mm, which gives a fluence 0.7 mJ/cm² per pulse. The probe beam detects the longitudinal (in the optical plane) component of the magnetization of the FM using a polarizer-analyzer scheme. The probe beam is polarized when incident on the sample and the analyzer is set to approximately 1 degree crossed with the incident probe beam. The measurements were made at room temperature.

III. RESULTS AND ANALYSIS

Figure 2 are a representative set of experimental results for the Kerr signal as a function of pump-probe delay for two samples with different Co thickness and H_{EB} . Typically there is a spike at the pump-probe overlap which is due to the heating of the electron gas and exchange of heat into the lattice. This process lasts < 5 ps, and in the plots in Fig. 2 do not show the spike because the step size used during the experiment is too big to resolve the quick decay. After the temperature in the lattice has equilibrated, the pump-probe signal oscillates and decays as a function of probe delay. The oscillations are single frequency, as illustrated by the fits in Figure 2 to a damped sinusoidal. From these fits, a frequency for oscillation can be extracted. The frequency does not

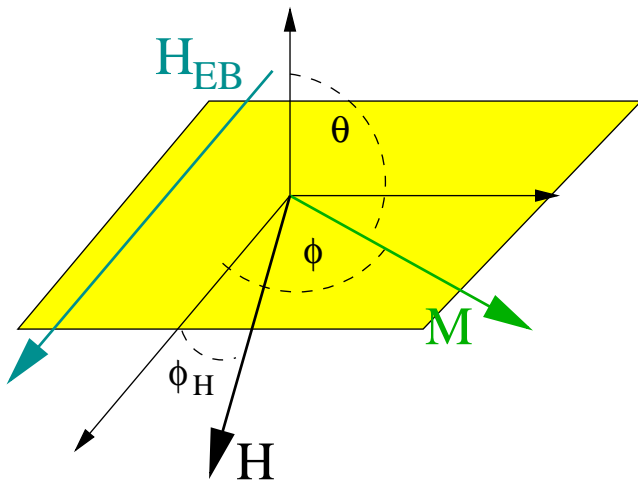


FIG. 3: Coordinates used in the FMR model. The θ and ϕ are the typical polar coordinates. H_{EB} is assumed to be along the x-axis, and H and M are assumed to be in the xy-plane, which is the plane of the film.

appear to be strongly dependent on H_{EB} .

To describe the magnetization oscillations, we take the approach of FMR using the undamped Landau Lifshitz (LL) equation:

$$\frac{d\vec{M}}{dt} = -\gamma(\vec{M} \times \vec{H}) \quad (1)$$

Where \vec{M} is the magnetization of the sample, γ is the gyromagnetic ratio, and \vec{H} is a vector sum of all of the fields in the system, including exchange bias field, applied field, and any anisotropy fields. Typically the oscillation frequency is determined in FMR theory by considering the free magnetic energy of the system by taking into account all anisotropies and external fields:

$$F = -HM \cos(\phi - \phi_H) \sin \theta - H_{EB}M \cos \phi \sin \theta + 2\pi M' M \cos^2 \theta \quad (2)$$

Where the first term is the Zeeman interaction of the magnetization with the applied field, the second term is the interaction of the magnetization with the exchange bias field, and the third term is the demagnetization field, which points perpendicular to the film plane. Here the θ and ϕ are the polar coordinates of the magnetization, ϕ_H is the angle of the applied field from the exchange bias axis, assumed to be in the \hat{x} direction. A diagram of the coordinate system used in the calculation is in Figure 3.

The first derivatives of the free energy with respect to the polar angles determine the steady state direction of the magnetization:

$$\frac{\partial F}{\partial \theta} = 0 \quad \frac{\partial F}{\partial \phi} = 0 \quad (3)$$

The frequency can then be calculated using:

$$\omega = \frac{\gamma}{M \sin \theta} \left\{ \frac{\partial^2 F}{\partial^2 \theta} \frac{\partial^2 F}{\partial^2 \phi} - \left(\frac{\partial F}{\partial \theta \partial \phi} \right)^2 \right\}^{\frac{1}{2}} \quad (4)$$

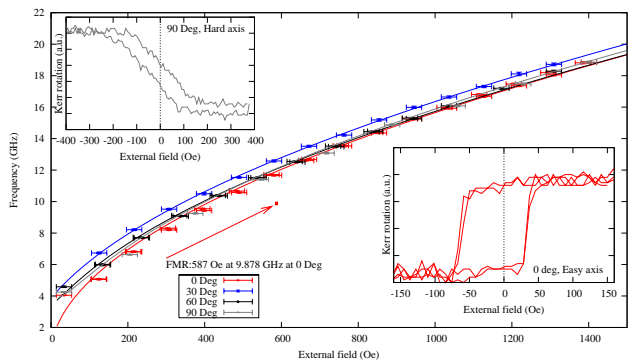


FIG. 4: Oscillation frequencies from the fits in Fig. 2 versus applied field for IrMn/250 Å Co and IrMn/120 Å Co for different angles between the applied field and H_{EB} . Inset are the MOKE curves for the hard axis and easy axis. A FMR measurement for the easy axis is also shown for comparison.

TABLE I: Exchange bias, demagnetization, and g values as extracted from the fits to the oscillation data using Eq. 3 and Eq. 4.

sample	H_{EB} (Oe)	H_D (Oe)	g
120 Å	106	27294	2.1
250 Å	49	27464	2.1

Equation 3 can then be used to fit the frequencies and Eq. 4 can be used to determine the magnetization direction for different applied fields. The free parameters are the exchange bias field and demagnetization field, along with g , which appears in the gyromagnetic ratio $\gamma = g1.76 \times 10^7/2$ Hz/Oe.

Figure 4 shows the oscillation frequencies versus applied field for the 250 Å sample at different angles between H_{EB} and H . The insets in the figure are hysteresis loops taking using MOKE on the easy ($\phi_H = 0$ degrees) and hard ($\phi_H = 90$ degrees) axis measurements. In addition there is a point taken from a FMR scan shown in red. This point corresponds to the 0 degree case, also shown in red.

Figure 5 shows the oscillation frequencies vs applied field for the 120 Å sample for different angles between the applied field H and H_{EB} . As in Fig. 4 the MOKE curves are inset with a FMR point for comparison in red. The angles here are obtuse but they can be thought of as acute angles with a magnetic field applied in the negative direction.

Table I summarizes the exchange bias, demagnetization, and g values from the fitting parameters. For comparison, the values for H_{EB} from hysteresis are 25 Oe for 250 Å and 67 Oe for 120 Å. The demagnetization field measured in the bulk is 17800 Oe. The accepted value of g in most systems varies between 2 and 2.1.

What is surprising in Figs. 2, 4, and 5 is that the oscillations persist even after the magnetization is saturated, as shown by the hysteresis loops inset in Figs 4 and 5.

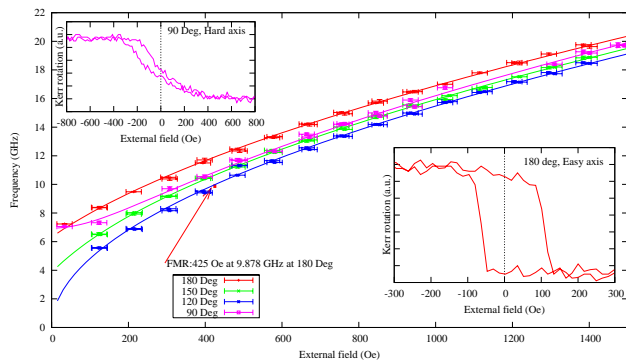


FIG. 5: Oscillation frequencies with fits for a sample of IrMn/120 Å Co for different angles between H_{EB} and H . The fits are shown in the same color as the points. The MOKE curves showing the easy (180 degrees) and hard (90 degrees) axis curves are shown. A single FMR measurement against the 180 degree (easy axis) curve is shown in red.

For example, the hard axis hysteresis loop inset on Fig. 4 shows that the magnetization is completely saturated at 250 Oe. The saturated state of the magnetization is the lowest energy state, and it is energetically unfavorable for the magnetization to rotate. In addition, with the magnetization saturated, there is no possibility of the ‘kick’ In the case of Ju et. al. and Weber et. al. the oscillations disappear, but in our case the oscillations persist, up through 1500 Oe.

We are currently exploring two explanations for this phenomenon. The first is that the pump laser pulse could

be disordering the AF under layer as seen recently by Duong et. al.¹² on the AF NiO. Their work shows a re-orientation of the Ni^{2+} between the original configuration and 90 degrees from the original induced by an intense laser pulse. The Ni^{2+} ion oscillates between the two configurations. If this was the case in our system, as the exchange bias recovered from the laser pulse the spins in the antiferromagnet would be oscillating which would induce precession in the ferromagnet.

The other possibility we are investigating is the work by Hase et. al.³ on NiFe/Cu/Co/IrMn spin valves that show that although IrMn is an antiferromagnet, it still has a small magnetic moment. This moment could provide enough of a stray field to cause the ‘kick’ discussed earlier.

In summary, we have detected coherent spin waves in an exchange biased system IrMn/Co, with two different Co thicknesses. The oscillations are single frequency and occur at all applied fields and angles between the exchange bias axis and applied field. We fit them using FMR theory, and the fits yield an exchange bias which is comparable to the hysteresis loop measurements. Work is ongoing to understand how we are able to excite these spin waves even though the magnetization is saturated.

Acknowledgments

The authors would like to thank Hailong Huang for providing a program to fit data and fruitful discussions, William Egelhoff Jr. and Li Gan for providing samples, and Jim Rantschler for providing FMR measurements.

* Electronic address: keoki@camelot.physics.wm.edu

¹ T. Gerrits, H. A. M. van der Berg, J. Hohlfield, L. Bar, and T. Rasing, *Nature* **418**, 509 (2002).

² J. Nogués and I. K. Schuller, *J. Magn. Mater.* **192**, 203 (1999).

³ T. P. A. Hase, B. D. Fulthorpe, S. B. Wilkins, B. K. Tanner, C. H. Marrows, and B. J. Hickey, *Appl. Phys. Lett.* **79**, 985 (2001).

⁴ S. F. Cheung and P. Lubitz, *J. Appl. Phys.* **87**, 4927 (2000).

⁵ G. Ju, A. V. Nurmikko, R. F. C. Farrow, R. F. Marks, M. J. Carey, and B. A. Gurney, *Phys. Rev. Lett.* **82**, 3705 (1999).

⁶ G. Ju, L. Chen, A. V. Nurmikko, R. F. C. Farrow, R. F. Marks, M. J. Carey, and B. A. Gurney, *Phys. Rev. B* **62**, 1171 (2000).

⁷ M. van Kampen, C. Jozsa, J. T. Kohlhepp, P. LeClair, L. Lagae, W. J. M. de Jonge, and B. Koopmans, *Phys. Rev. Lett.* **88**, 227201 (2002).

⁸ B. Hillebrands and J. Fassbender, *Nature* **Nature**, 493 (2002).

⁹ J. Hohlfield, E. Matthias, R. Knorren, and K. H. Benneman, *Phys. Rev. Lett.* **78**, 4861 (1997).

¹⁰ M. R. Freeman, M. J. Brady, and J. Smyth, *Appl. Phys. Lett.* **60**, 2555 (1992).

¹¹ M. C. Weber, H. Nembach, and J. Fassbender, *J. Appl. Phys.* **95**, 6613 (2004).

¹² N. P. Duong, T. Satoh, and M. Fiebig, *Phys. Rev. Lett.* **95**, 117402 (2004).